ARMY RESEARCH LABORATORY

Performance and Evaluation of Bipolar Fuel Cell Stacks

Deryn Chu, Rongzhong Jiang, Charles Walker, Richard Jacobs, Krist Gardner, and Jim Stephens

ARL-TR-2064 February 2000

Approved for public release; distribution unlimited.

Army Research Laboratory

Adelphi, MD 20783-1197

ARL-TR-2064 February 2000

Performance and Evaluation of Bipolar Fuel Cell Stacks

Deryn Chu, Rongzhong Jiang, Charles Walker
Sensors and Electron Devices Directorate, ARL

Richard Jacobs, Krist Gardner, and Jim Stephens
Power Sources Division, U.S. Army CECOM

Abstract

Under a joint technology planning annex (TPA) agreement, fuel cell groups at the U.S. Army Research Laboratory (ARL) and the U.S. Army Communications-Electronics Command (CECOM) worked together to develop Army power sources for soldier applications. Two 50-W bipolar fuel cell stacks designed by CECOM were extensively evaluated. The performance of the stacks depended significantly on the environmental temperature. Decreasing environmental temperature granted better heat dissipation in the stacks, resulting in improved stack performance. Long-term performance of 62 W was obtained at low temperature (–5 °C). Higher environmental temperatures caused an increase in stack surface temperature. When the stack surface temperature reached 43 °C, the stack voltage dropped to zero within a short time. The maximum power density for long-term operation was 97.3 W/kg, or 167 W/L. The average hydrogen utilization efficiency was 95 percent. The water production efficiency was dependent on the discharge currents, varying from 40 percent (at 1.0 A) to 90 percent (at 2.5 A).

Contents

Figures

Tables

1. Introduction

A fuel cell is an electrochemical device that directly converts the chemical energy of the reactants, a fuel and an oxidant, into electrical power [1,2]. A fuel cell will continue to operate as long as the externally stored reactants are supplied. Fuel cells are more efficient than combustion technology, partly because they avoid the Carnot cycle limitation. Since a fuel cell generates electricity without combustion, it does not produce the air pollutants that are byproducts of the combustion process. Similar to an internal combustion engine, and unlike a battery, a fuel cell does not require recharging—it will provide power indefinitely, as long as fuel is supplied.

The basic H_2/air polymer electrolyte membrane fuel cell (PEMFC) consists of (a) an anode (carbon-supported platinum black), (b) an electrolyte (Nafion), and (c) a cathode (carbon-supported platinum black). Nafion is a cation-exchange polymer membrane that has a perfluorinated polymer backbone with sulfonic acid substituents that are periodically attached. Nafion exhibits exceptionally high electrochemical, thermal, and chemical stability in fuel cell environmental conditions. In order to achieve high voltage and high power, a huge number of single cells are assembled together to act as a power source in practical applications. Such an assembly is called a fuel cell stack.

For an H_2/O_2 fuel cell, hydrogen would become oxidized at the anode via the half reaction

$$H_2 \longrightarrow 2H^+ + 2e^- \qquad E^0 = 0\ \mathrm{V}\ , \tag{1}$$

whereas oxygen would become reduced at a cathode via the reaction

$$O_2 + 4H^+ + 4e^- \longrightarrow 2\,H_2O \qquad E^0 = 1.23\ \mathrm{V}\ . \tag{2}$$

The overall reaction is

$$2H_2 + O_2 \longrightarrow 2\,H_2O \qquad E^0 = 1.23\ \mathrm{V}\ . \tag{3}$$

The net result is the generation of electricity, heat, and water, as shown in equation (3).

PEMFCs are the most desirable portable power supply device, primarily because they are lightweight and have a high power density. A PEMFC power source is being developed for a wide variety of applications that now use batteries, from laptop computers to electric vehicles [3–8]. A PEMFC system can be used with a replaceable fuel cartridge (e.g., tanked/metal or chemical hydrides) for practical operations without any environmental concern. Small fuel cell systems, if successfully developed, can replace batteries by directly providing power.

Future man-portable power sources systems will need high power density and a long operating life, and they will have to be small and lightweight. Using a lightweight PEMFC stack as a portable power source can reduce the physical burden on the carrier. Several key areas need to be addressed to successfully produce the desired high-performance, lightweight, ambient-temperature and -pressure fuel-cell system [9–14]: (1) thermals and heat transfer management, (2) water management, (3) environmental factors, (4) hydrogen storage conditions, (5) determination of the best optimum stoichiometry of fuel and oxidant, and (6) system integration for high-performance PEMFCs.

Fuel cell groups from the U.S. Army Research Laboratory (ARL) and the U.S. Army Communications-Electronics Command (CECOM) worked together on a PEMFC project under a joint technology planning annex (TPA) agreement (TPA SE-CE-O2-98). In this report, we give performance evaluation results for the bipolar fuel cell stacks. Two identical 50-W bipolar fuel cell design stacks (CECOM tags 764 and 762) were evaluated.

2. Experiment

In this experiment, high-purity hydrogen (99.99%) was used as the fuel and compressed air as an oxygen source. The environmental temperature was controlled by a Tenney environmental chamber (model BTRC), which was programmed through a computer with Linktenn II software. An Arbin battery tester (BT-2043) was used to administer constant current discharge tests. A Hewlett-Packard electronic load (model 6050A) and multimeter were used to measure current and voltage when the stack voltage was greater than 35 V. A Matheson digital flowmeter (LFE 1000H) was used to measure hydrogen flow, and a hydrogen purger was set to purge for 10 s every 5 min during all measurements. The inlet hydrogen and air pressures were adjusted to 3 and 5 psi, respectively. An ac electric fan (~10 W) was pointed toward the stack during testing to dissipate excess heat. A thermocouple was attached to the top surface of the stack to measure stack surface temperature.

CECOM provided two identical fuel cell stacks for evaluation (CECOM tags 764 and 762). CECOM did not relate the nominal voltage and power ratings. Each stack contained 42 single cells connected in series. The dry stack weight was 637 g, and the wet stack weight (after humidification) was 643 g. (The stacks were humidified before evaluation.) The electrode area was about 17.6 cm^2 (4.0 × 4.4 cm). The dimensions of the stack are given in figure 1.

Figure 1. Dimensional drawing of 50-W fuel cell stack (42 cells, CECOM 762 or 764). Dry weight (before electrolyte membrane was humidified): 637 g (including two electric wires and two H_2 tubes, and excluding air or water tubes); wet weight (after membrane was humidified): 643 g.

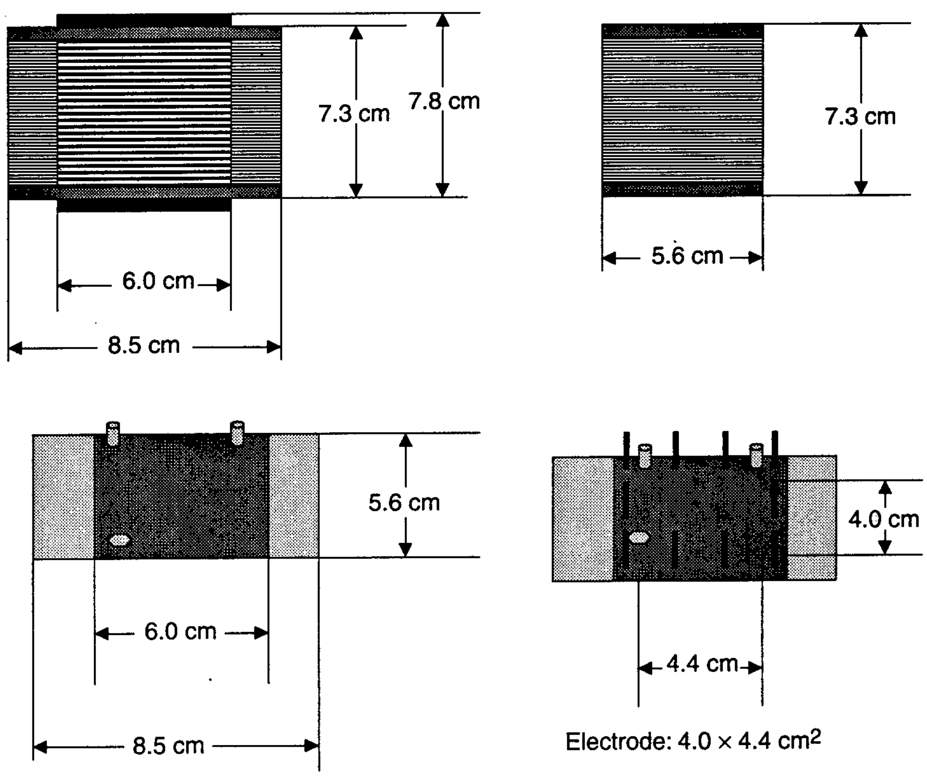

3. Results and Discussion

3.1 CECOM Fuel Cell Stack Tag 764

3.1.1 *Stack Performance*

Figure 2 shows the polarization curves for the fuel cell stack at 10 °C, fed with dry H_2 and dry air at different discharge currents. The open circuit voltage was about 42 V. Initially, the stack power output increased at low currents and plateaued at currents higher than 2 A; then it decreased at currents higher than 2.5 A. This behavior is probably caused by incomplete hydration of the electrolyte membrane. The maximum power output is approximately 50 W. As operating time and current increased, the membrane became more hydrated and stack performance improved significantly. Maximum power output was obtained at currents of 3.0 A (~67 W), and plateaus at currents higher than 3 A.

Figure 3 shows the stack performance at 10 and 20 °C environmental temperatures, under different discharge currents. Performance at 10 °C is slightly better than that at 20 °C.

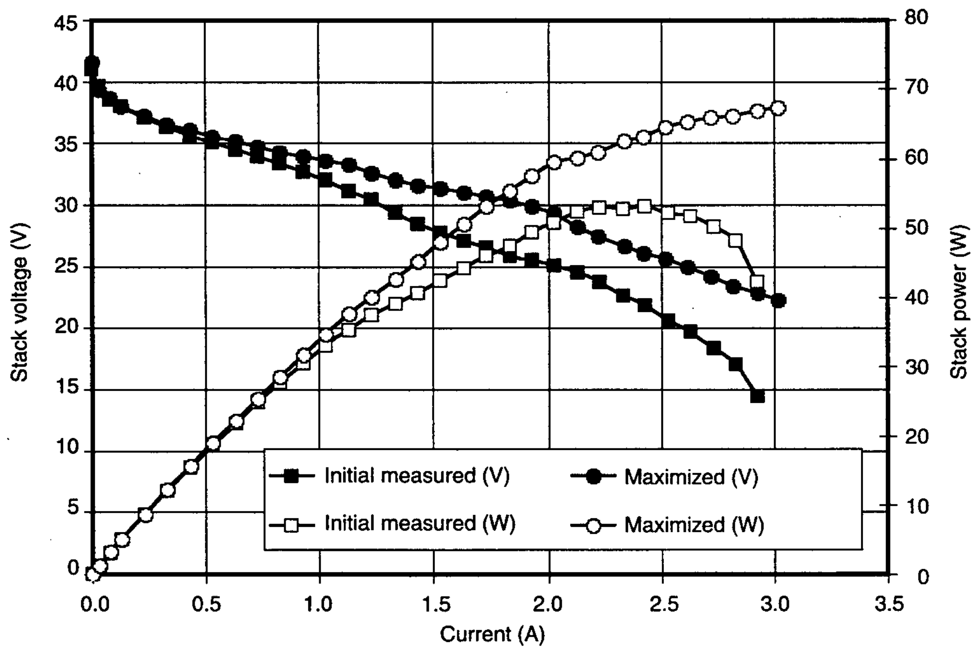

Figure 2. Discharge performance improving with electrolyte membrane humidification until reaching maximized performance for 50-W fuel cell stack (CECOM 764) at 10 °C. Dry air and dry H_2 fill; H_2 pressure = 3 psi; air pressure = 5 psi; H_2 purging: 10 s/5 min.

Figure 3. Discharge performance of 50-W fuel cell stack (CECOM 764) at different temperatures. Dry air and dry H_2 fill; H_2 pressure = 3 psi; air pressure = 5 psi; H_2 purging: 10 s/5 min.

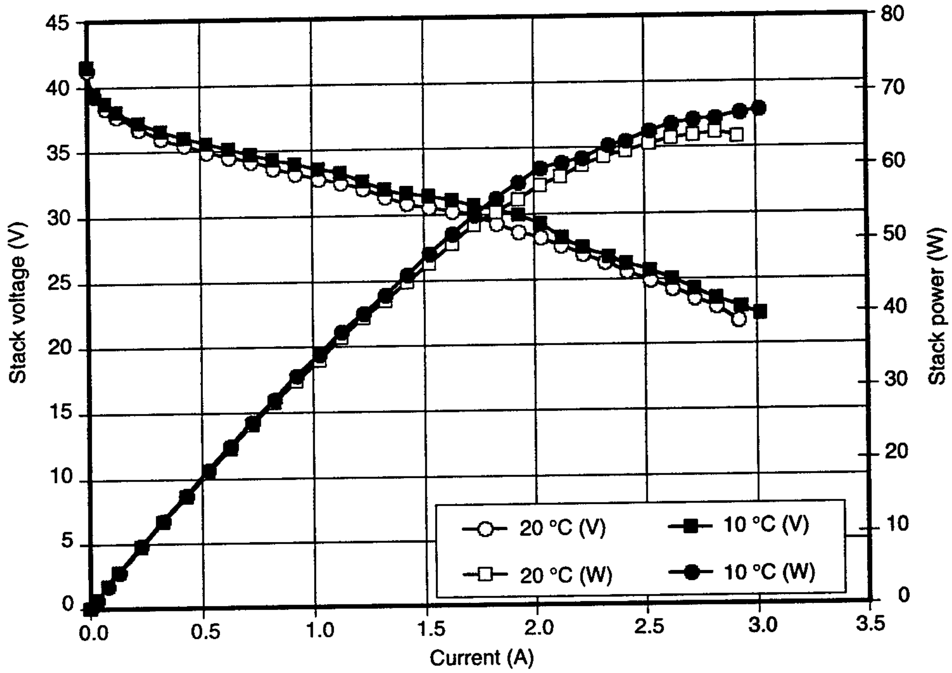

3.1.2 *Optimizing Fuel Cell Stack Performance*

Based on the stack performance results given in figures 2 and 3, various constant discharge currents at different environmental temperatures (from –5 to 30 °C) were performed for longer (2-hr) evaluation periods.

Effect of temperature during constant discharge current.—Figure 4 shows the stack performance under constant discharge current (I = 1.0 A) at different temperatures. At lower temperature (10 °C), the stack has a lower initial voltage; however, the long-term performance of the stack at 10 and 20 °C is almost identical. Approximately 32 W output was obtained at 1.0 A constant current discharge. At 30 °C, the stack has good performance during the first ~20 min, after which the voltage rapidly drops to zero within 40 min. In order to understand the reason for the poor performance at 30 °C, we monitored the stack surface temperature during operation. Figure 5 shows the stack surface temperatures at different currents and environmental temperatures; the stack surface temperatures increase significantly with increasing discharge current and environmental temperature. At 1.0 A and 30 °C environmental temperatures, the stack surface temperature is as high as 43 °C. Undoubtedly, the temperature inside the stack would be much higher than 43 °C, causing the electrolyte membrane to dehydrate, which would result in a large stack voltage drop.

Figure 4. Constant current discharge (I = 1.0 A) performance of 50-W fuel cell stack (CECOM 764) at different environmental temperatures. H_2 inlet pressure = 3 psi; air inlet pressure = 5 psi; H_2 purging: 10 s/5 min; cooling by fan; dry H_2 and dry air fill.

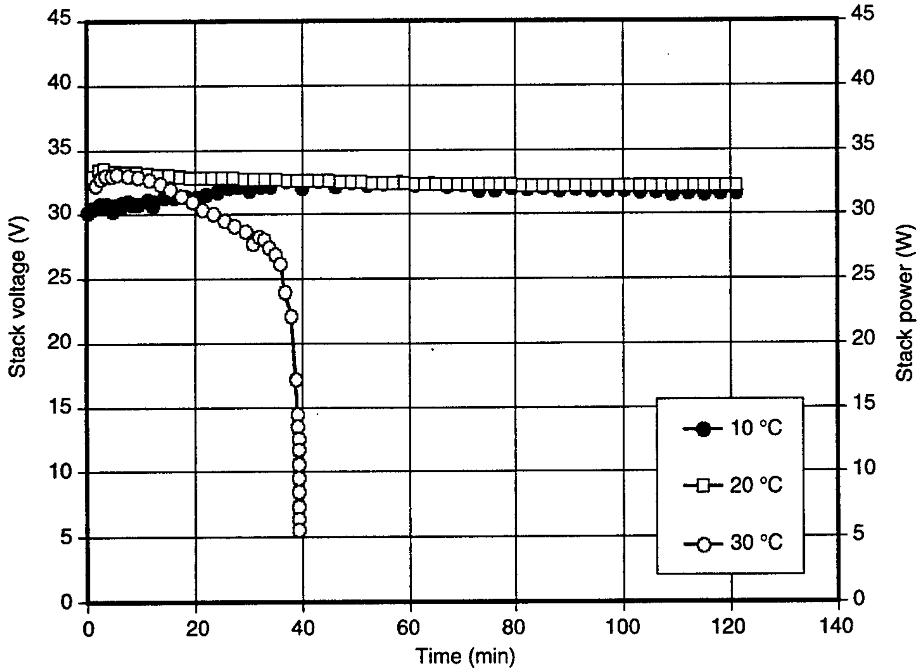

Figure 5. Effect of discharge on stack surface temperature at various environmental temperatures for 50-W fuel cell stack (CECOM 764).

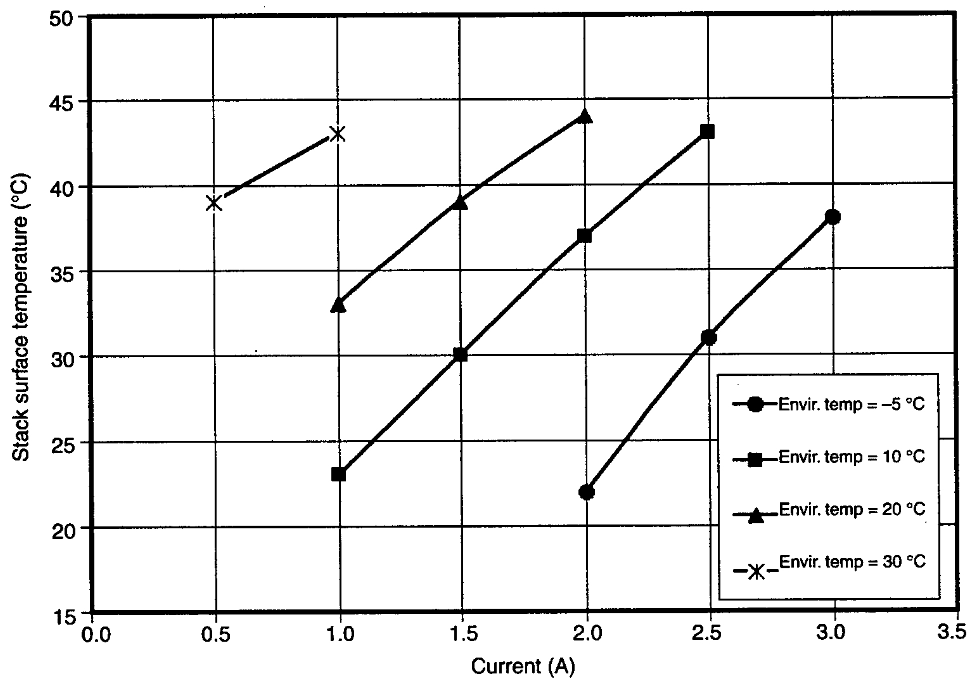

Effect of temperature at different discharge currents.—Figure 6(a) shows the voltage versus time plots for constant current discharge at 30 °C. At 0.5 A discharge current, the voltage was very stable and lasted more than 120 min. The stack voltage decreased slightly after over the first 40 min and then stabilized. For a discharge current of 1 A, the stack voltage dropped very fast, reaching zero in only about 40 min. The corresponding power versus time plot is shown in figure 6(b). A 16-W output was

Figure 6. Constant current discharge performance of 50-W fuel cell stack (CECOM 764) at 30 °C: (a) voltage vs time and (b) power vs time. H_2 inlet pressure = 3 psi; air inlet pressure = 5 psi; H_2 purging: 10 s/5 min; cooling by fan; dry H_2 and dry air fill.

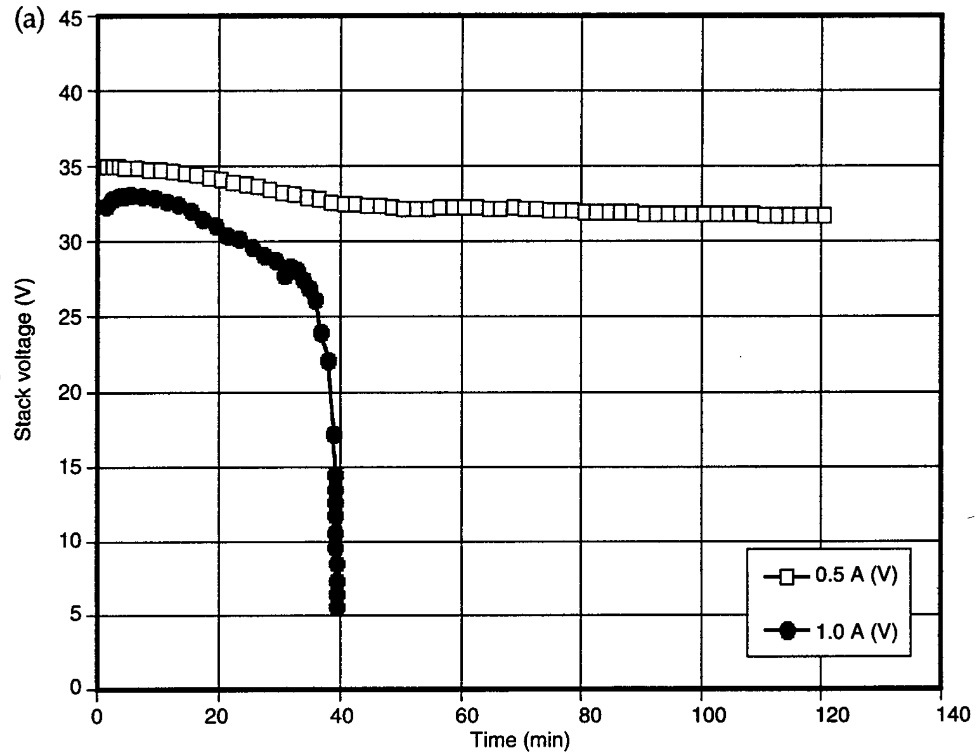

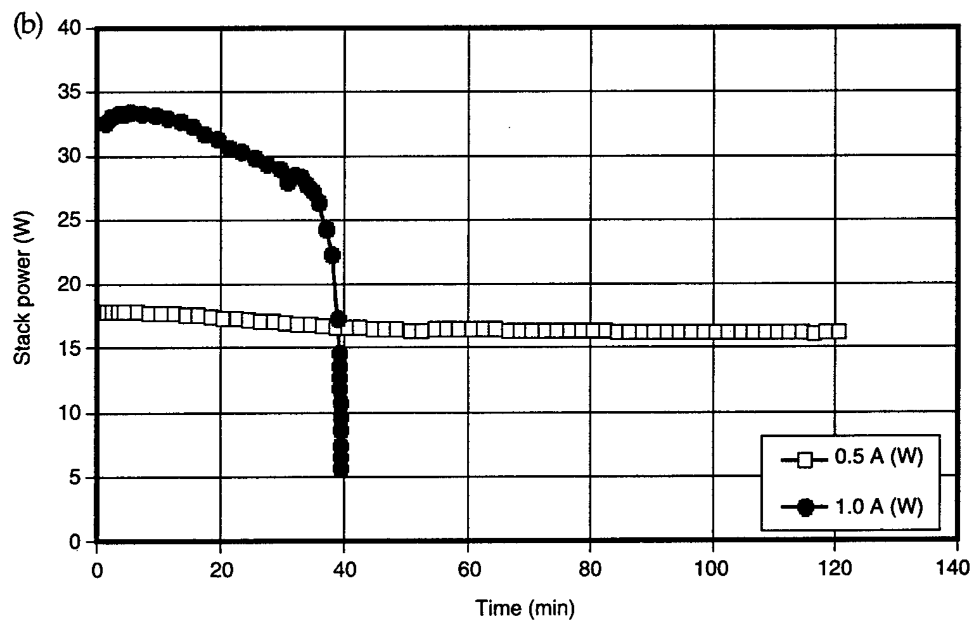

obtained at 0.5 A and 30 °C environmental temperature. Figure 7(a) shows the voltage versus time plot for constant current discharge at 20 °C. Compared with the results at 30 °C, the performance of the stack was much improved. At 1.0 and 1.5 A discharge currents, the stack voltage was stable for the entire test period. However, when the discharge current was increased to 2.0 A, the voltage dropped again. From the data shown in figure 5, we know that the stack surface temperature had increased to 44 °C at 2.0 A. At this temperature, the membrane electrolyte was

Figure 7. Constant current discharge performance of 50-W fuel cell stack (CECOM 764) at 20 °C: (a) voltage vs time and (b) power vs time. H_2 inlet pressure = 3 psi; air inlet pressure = 5 psi; H_2 purging: 10 s/5 min; cooling by fan; dry H_2 and dry air fill.

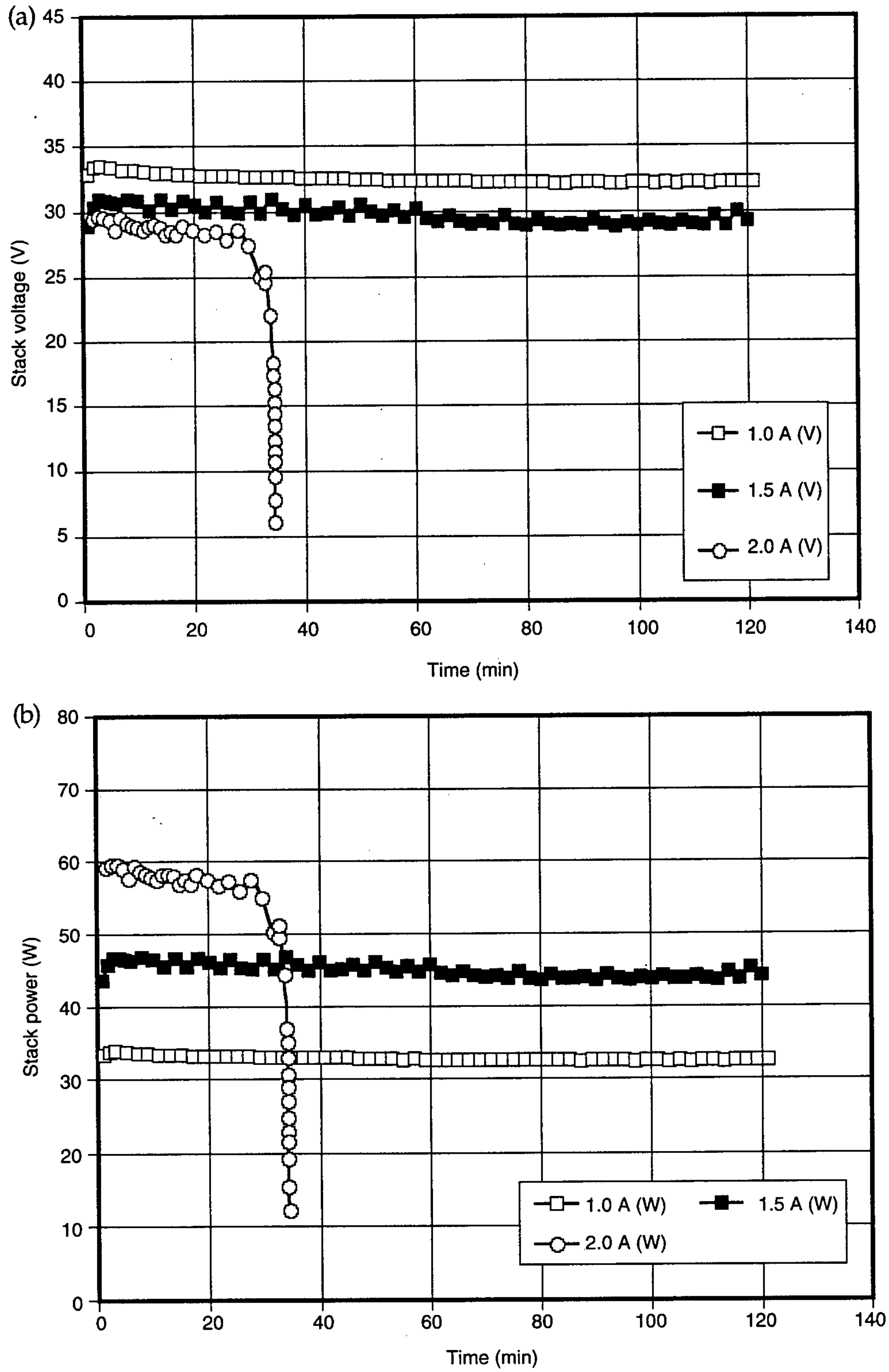

dehydrated. Figure 7(b) shows the corresponding power versus time plots. The stable stack power outputs were 44 and 33 W for 1.5 and 1.0 A, respectively. Figure 8(a) shows the stack voltage versus time plots for different constant current discharges. Even when the discharge current increases to 2.0 A, the stack could maintain stable discharge performance.

Figure 8. Constant current discharge performance of 50-W fuel cell stack (CECOM 764) at 10 °C: (a) voltage vs time and (b) power vs time. H_2 inlet pressure = 3 psi; air inlet pressure = 5 psi; H_2 purging: 10 s/5 min; cooling by fan; dry H_2 and dry air fill.

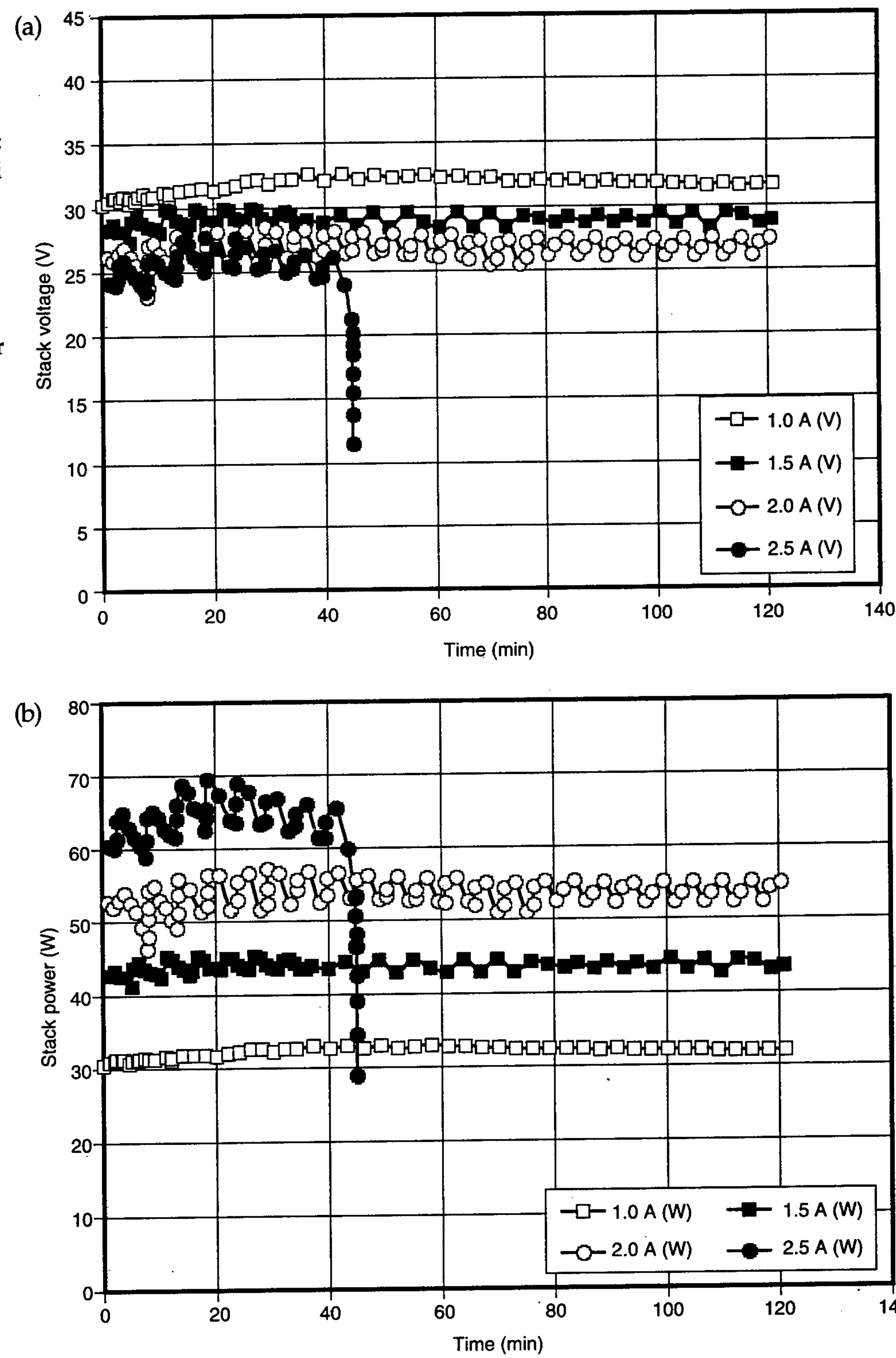

However, stack performance dropped at 2.5 A discharge current. The data from figure 8(a) are also plotted for power versus time in figure 8(b). Approximately 55 W constant performance was obtained at a current of 2.0 A. However, when the discharge current was increased to 2.5 A, the stack power dropped off within 45 min. Based on the results shown in figures 6 to 8, we expected the stack performance to improve at lower temperatures. Figure 9(a) shows the voltage versus time plots for constant current discharge at –5 °C. Stack performance was very stable up to a current of 2.5 A, but failed at a discharge current of 3 A. Figure 9(b) shows the corresponding power versus time plots. An approximately 62-W

Figure 9. Constant current discharge performance of 50-W fuel cell stack (CECOM 764) at –5 °C: (a) voltage vs time and (b) power vs time. H_2 inlet pressure = 3 psi; air inlet pressure = 5 psi; H_2 purging: 10 s/5 min; cooling by fan; dry H_2 and dry air fill.

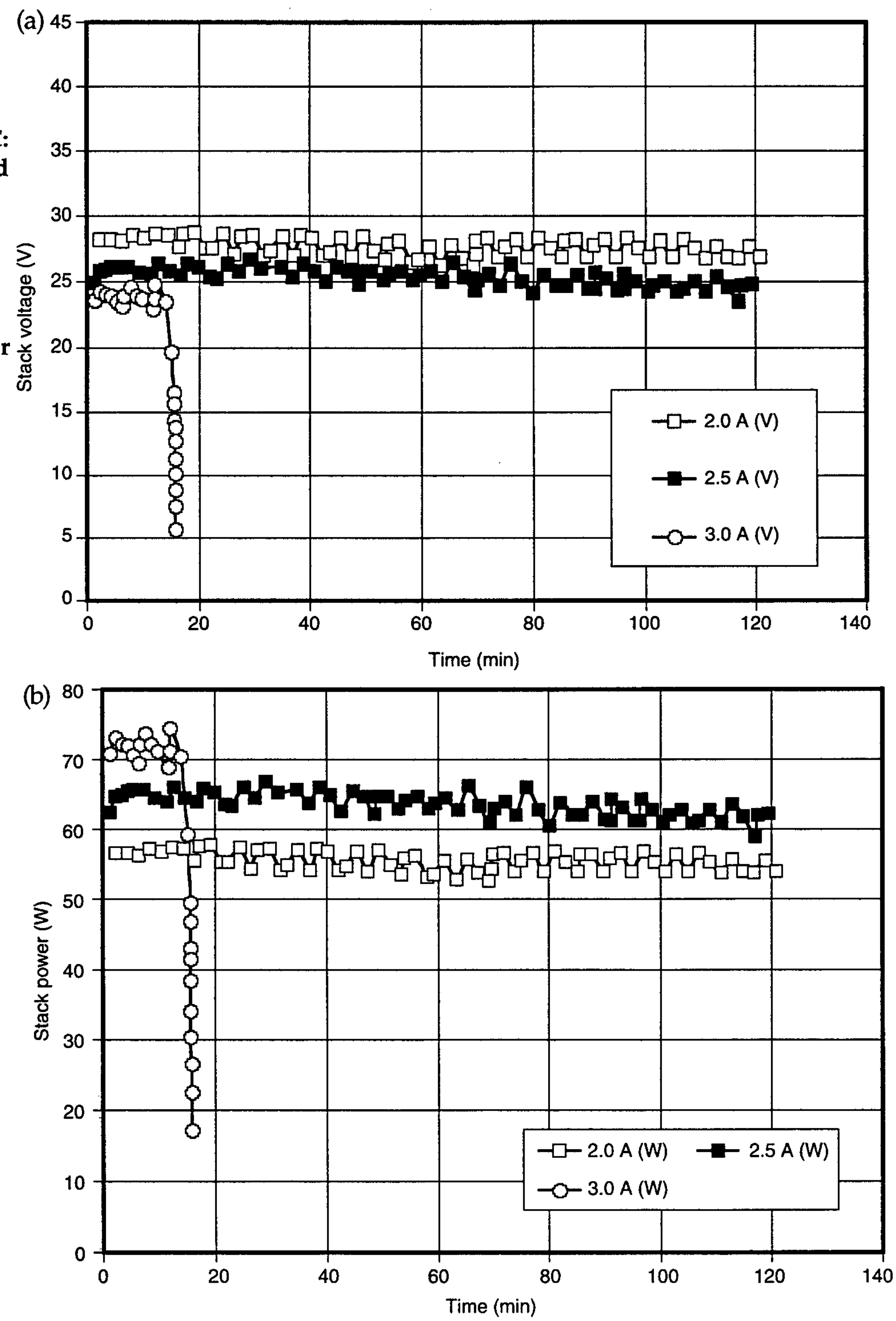

constant output was obtained at 2.5 A during the entire 120-min experiment. When discharge current was increased to 3.0 A, the stack power dropped to zero within 20 min. Many problems (for example, with heat dissipation, water management, and supplies of oxygen and hydrogen) may occur as a consequence of high discharge current (3 A).

3.1.3 *Hydrogen Utilization Efficiency*

Figure 10 shows that the effect of discharge current on hydrogen flow rates is linear. It also shows the efficiency of hydrogen utilization: the hydrogen utilization efficiency was approximately 95 percent for discharge currents of 1.0 A and above.

3.1.4 *Water Production Efficiency*

Figure 11(a) shows the effect of environmental temperature on water production efficiency, which increased only slightly from –5 to 20 °C. Figure 11(b) shows that an increase in discharge current increased water production efficiency.

Figure 10. Effect of current on H_2 flow rate and H_2 efficiency for 50-W fuel cell stack (CECOM 764, containing 42 single cells connected in series).

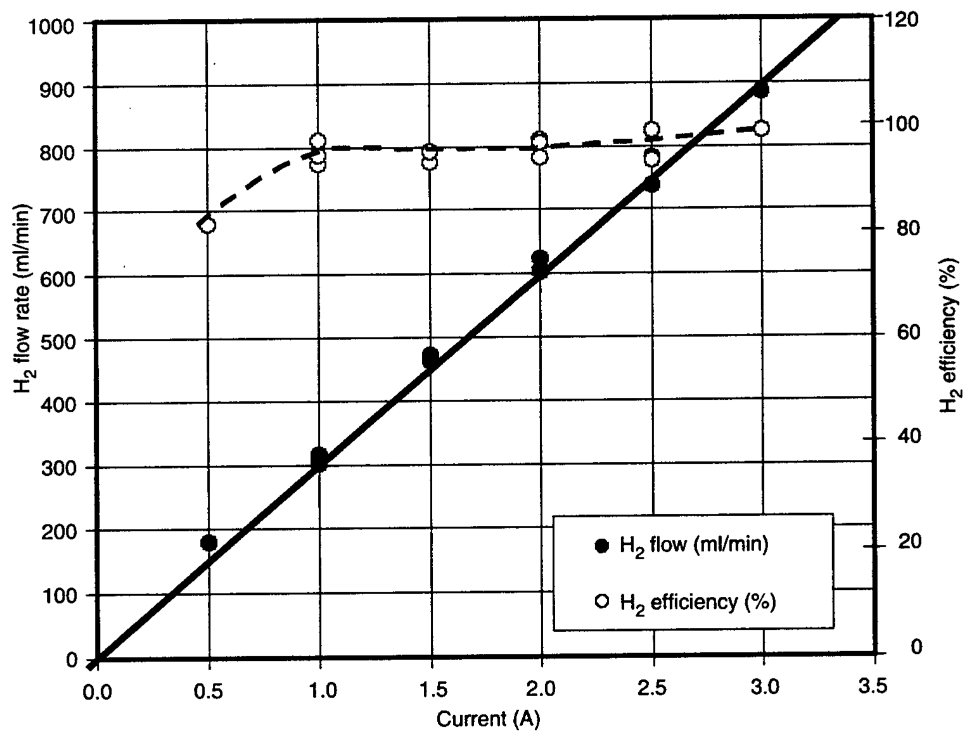

Figure 11. Effect of (a) environmental temperature (at 2.0 A discharge) and (b) discharge current (at 10 °C environmental temperature) on product water efficiency for 50-W fuel cell stack (CECOM 764).

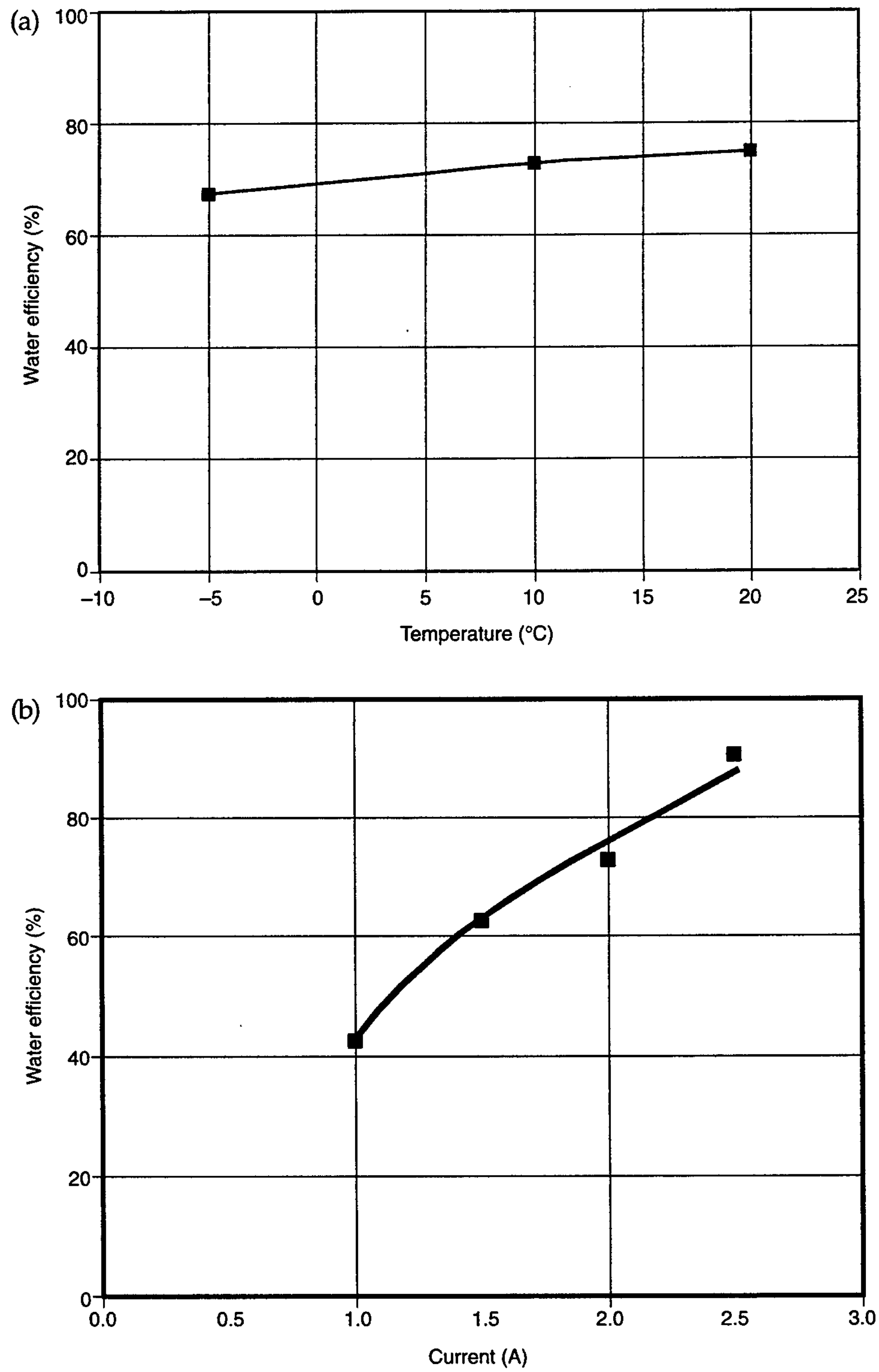

3.2 CECOM Fuel Cell Stack Tag 762

This stack leaked during evaluation, so only limited data were obtained.

3.2.1 *Stack Performance*

Figure 12 shows a polarization curve for the fuel cell stack at 25 °C. The open circuit voltage was approximately 42 V. Because of poor heat dissipation, which caused the electrolyte membrane to dehydrate, the voltage-current curve decreased significantly at currents greater than 1.0 A. The maximum power output was approximately 39 W.

3.2.2 *Constant Current Discharge*

Figure 13(a) shows voltage versus time plots for three different discharge currents for the fuel cell stack at 25 °C. At 1.0 A discharge current, the stack voltage was very stable. When the discharge current increased to 1.25 A, the voltage decreased a little with time. At 1.5 A discharge current, the stack voltage dropped very fast within 20 min. Figure 13(b) shows the corresponding stack power versus time plots at the same three discharge currents: at 1.0 A and 25 °C, a stable power output of approximately 33 W was obtained.

Figure 12. Discharge performance of 50-W fuel cell stack (CECOM 762) at 25 °C. Dry air and dry H_2 fill; H_2 pressure = 3 psi; air pressure = 5 psi; H_2 purging: 10 s/5 min; at 2.03 A, stack temperature increased to 52 °C.

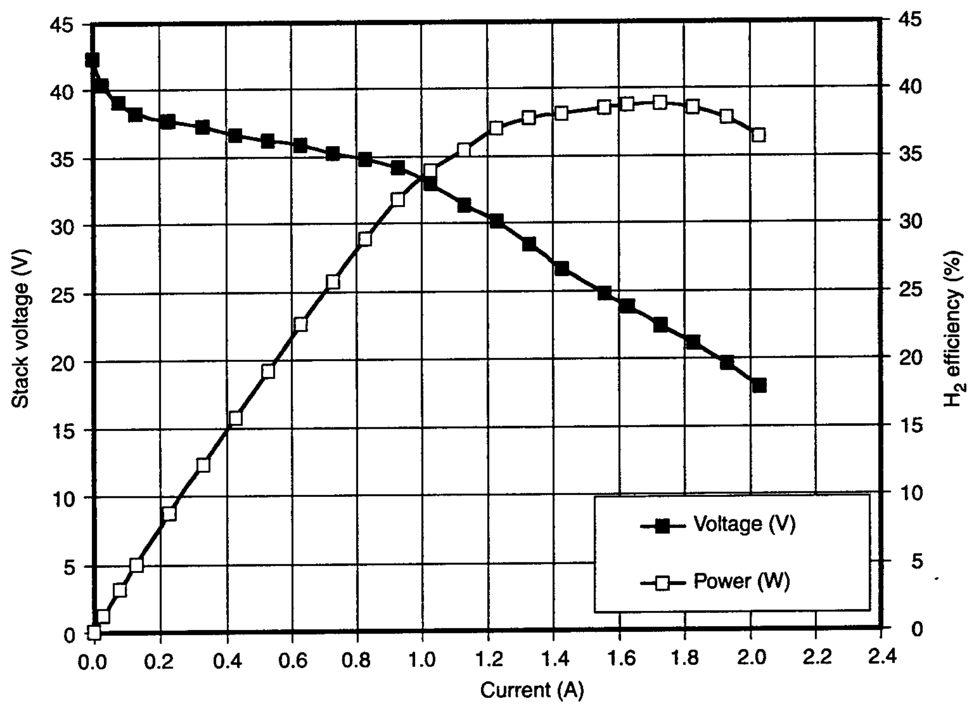

Figure 13. Constant current discharge performance of 50-W fuel cell stack (CECOM 762) at 25 °C and 64% humidity: (a) voltage vs time and (b) power vs time. H_2 inlet pressure = 3 psi. Air inlet pressure = 5 psi. H_2 Purging: 10 s/5 min. Cooling by fan. Dry H_2 and dry air fill.

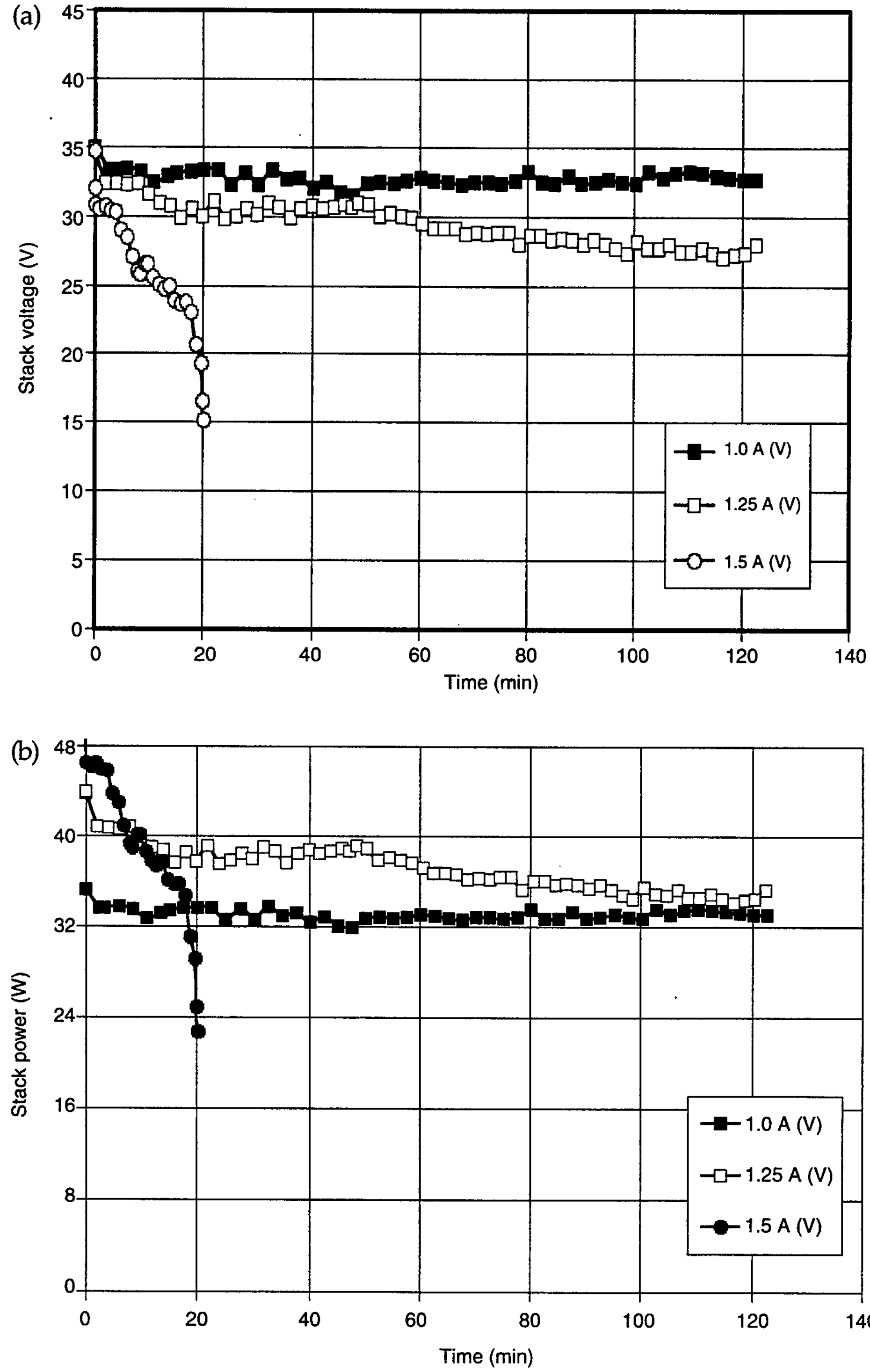

4. Conclusions

The 50-W bipolar fuel cell stack was extensively evaluated under various constant discharge currents at different environmental temperatures. The effects of environmental temperatures on the maximum stable power outputs are summarized in table 1. A 62-W long-term performance was obtained at low environmental temperature (–5 °C). As environmental temperature was increased, the stack surface temperature increased proportionally, causing heat to dissipate from the stack. When the stack surface temperature reached 43 °C, the stack voltage dropped significantly within a short time. The effect of environmental temperatures on the minimum discharge current—causing the stack voltage to drop to zero as the stack temperature rises—is summarized in table 2. At 30 °C, stack performance was unstable at a current of 1.0 A. However, at –5 °C, stable performance was observed until a current of 3.0 A was reached. Improving heat dissipation efficiency will enhance the stack performance significantly.

Table 1. Effect of environmental temperature on maximum stable stack power output.

Environmental temperature (°C)	Maximum stable stack power (W)	Discharge current (A)	Stack surface temperature (°C)
–5	62	2.5	31
10	55	2.0	37
20	44	1.5	39
25	33	1.0	39
30	16	0.5	39

Table 2. Effect of temperature on minimum discharge current: causing stack voltage to drop to zero.

Environmental temperature (°C)	Minimum discharge current (A)	Stack surface temperature (°C)
–5	3.0	38
10	2.5	43
20	2.0	44
25	1.5	48
30	1.0	43

References

1. A. J. Apply and E. B. Yeager, *Energy* **11** (1986), 137.
2. D. Linden, *Handbook of Batteries and Fuel Cells*, McGraw-Hill, Inc. (1984), pp 41–43.
3. S. Srinivasan, E. A. Ticianelli, C. R. Derouin, and A. Redondo, *J. Power Sources* **22** (1988), 235.
4. K. Prater, *J. Power Sources*, **29** (1990).
5. M. S. Wilson and S. Gottesfeld, *J. Appl. Electrochem.* **22**, 1 (1992).
6. Guenther Scherer, "PEFC Research at Paul Scherrer Institute," *Proceedings of the IEA Workshop for the PEFC Annex*, 14–15 September 1992, Ottawa, Canada.
7. "How to Build a Clean Machine," *Business Week*, 27 May 1996.
8. "Detroit's Impossible Dream?" *Business Week*, 2 March 1998.
9. D. Chu, S. Gilman, and L. Jarvis, Electrochemical Society Meeting, Fall 1997.
10. D. Chu, R. Jiang, and Charles Walker, accepted for publication by *J. Appl. Electrochem.*
11. D. Chu and R. Jiang, *J. Power Sources* **80** (1999), 226–234.
12. D. Chu and R. Jiang, accepted for publication in *J. Power Sources*.
13. R. Jiang and D. Chu, 6th Grove Fuel Cell Seminar, September 1999.
14. D. Chu and R. Jiang, *Proc. J. Electrochem. Soc.* **PV 98-27**, 470.

Distribution

Admnstr
Defns Techl Info Ctr
Attn DTIC-OCP
8725 John J Kingman Rd Ste 0944
FT Belvoir VA 22060-6218

Ofc of the Secy of Defns
Attn ODDRE (R&AT)
The Pentagon
Washington DC 20301-3080

OSD
Attn OUSD(A&T)/ODDR&E(R) R J Trew
Washington DC 20301-7100

AMCOM MRDEC
Attn AMSMI-RD W C McCorkle
Redstone Arsenal AL 35898-5240

CECOM
Attn PM GPS COL S Young
FT Monmouth NJ 07703

CECOM Night Vsn/Elect Sensors Dirctrt
Attn AMSEL-RD-NV-D
FT Belvoir VA 22060-5806

Commander
CECOM R&D
Attn AMSEL-IM-BM-I-L-R Stinfo Ofc
Attn AMSEL-IM-BM-I-L-R Techl Lib
Attn AMSEL-IM-BM-I-L R Hamlen
FT Monmouth NJ 07703-5703

Deputy for Sci & Techlgy
Attn Ofc Asst Sec Army (R&D)
Washington DC 30210

AF Wright Aeronautical Labs
Attn R Marsh
AFWAL-POOS-2
Wright-Patterson AFB, OH 45433

Dir for MANPRINT
Ofc of the Deputy Chief of Staff for Prsnnl
Attn J Hiller
The Pentagon Rm 2C733
Washington DC 20301-0300

Hdqtrs
Attn DAMA-ARZ-D F D Verderame
Washington DC 20310

US Army ARDEC
Attn AMSTA-AR-TD M Fisette
Bldg 1
Picatinny Arsenal NJ 07806-5000

Commander
US Army CECOM
Attn AMSEL-RD-CZ-PS-B M Brundage
FT Monmouth NJ 07703-5000

US Army CECOM Rsrch Dev & Engrg Ctr
Attn AMSEL-RD-AS-BE E Plichta
FT Monmouth NJ 07703-5703

US Army Edgewood RDEC
Attn SCBRD-TD G Resnick
Aberdeen Proving Ground MD 21010-5423

US Army Info Sys Engrg Cmnd
Attn ASQB-OTD F Jenia
FT Huachuca AZ 85613-5300

US Army Natick RDEC Acting Techl Dir
Attn SSCNC-T P Brandler
Natick MA 01760-5002

US Army Simulation, Train, & Instrmntn
Cmnd
Attn J Stahl
12350 Research Parkway
Orlando FL 32826-3726

US Army Tank-Automtv Cmnd Rsrch, Dev, &
Engrg Ctr
Attn AMSTA-TA J Chapin
Warren MI 48397-5000

US Army Train & Doctrine Cmnd
Battle Lab Integration & Techl Dirctrt
Attn ATCD-B J A Klevecz
FT Monroe VA 23651-5850

Distribution (cont'd)

US Military Academy
Mathematical Sci Ctr of Excellence
Attn MDN-A LTC M D Phillips
Dept of Mathematical Sci Thayer Hall
West Point NY 10996-1786

Nav Rsrch Lab
Attn Code 2627
Washington DC 20375-5000

Nav Surface Warfare Ctr
Attn Code B07 J Pennella
17320 Dahlgren Rd Bldg 1470 Rm 1101
Dahlgren VA 22448-5100

Marine Corps Liaison Ofc
Attn AMSEL-LN-MC
FT Monmouth NJ 07703-5033

USAF Rome Lab Tech
Attn Corridor W Ste 262 RL SUL
26 Electr Pkwy Bldg 106
Griffiss AFB NY 13441-4514

DARPA
Attn S Welby
3701 N Fairfax Dr
Arlington VA 22203-1714

Hicks & Associates Inc
Attn G Singley III
1710 Goodrich Dr Ste 1300
McLean VA 22102

Palisades Inst for Rsrch Svc Inc
Attn E Carr
Attn Documents
1745 Jefferson Davis Hwy Ste 500
Arlington VA 22202-3402

US Army Rsrch Ofc
Attn AMSRL-RO-D C Chang
Attn AMSRL-RO-EN B Mann
PO Box 12211
Research Triangle Park NC 27709-2211

US Army Rsrch Lab
Attn AMSRL-CI-AS Mail & Records Mgmt
Attn AMSRL-CI-AT Techl Pub (3 copies)
Attn AMSRL-CI-LL Techl Lib (3 copies)
Attn AMSRL-D R W Whalen
Attn AMSRL-DD J Miller
Attn AMSRL-RO-PS R Paur
Attn AMSRL-SE J Pelligrino
Attn AMSRL-SE-D E Scannell
Attn AMSRL-SE-DC D Chu (25 copies)
Attn AMSRL-SE-DC S Gilman
Attn AMSRL-SE-DC R. Jiang
Attn AMSRL-SE-E J Mait
Attn AMSRL-SS
Adelphi MD 20783-1197

REPORT DOCUMENTATION PAGE

Form Approved
OMB No. 0704-0188

1. AGENCY USE ONLY *(Leave blank)*

2. REPORT DATE February 2000

3. REPORT TYPE AND DATES COVERED Progress, 10/98–9/99

4. TITLE AND SUBTITLE Performance and Evaluation of Bipolar Fuel Cell Stacks

5. FUNDING NUMBERS
DA PR: —
PE: 62120A

6. AUTHOR(S) Deryn Chu, Rongzhong Jiang, Charles Walker (ARL), Richard Jacobs, Krist Gardner, and Jim Stephens (Power Sources Division, U.S. Army CECOM)

7. PERFORMING ORGANIZATION NAME(S) AND ADDRESS(ES)
U.S. Army Research Laboratory
Attn: AMSRL-SE-DC email: dchu@arl.mil
2800 Powder Mill Road
Adelphi, MD 20783-1197

8. PERFORMING ORGANIZATION REPORT NUMBER
ARL-TR-2064

9. SPONSORING/MONITORING AGENCY NAME(S) AND ADDRESS(ES)
U.S. Army Research Laboratory
2800 Powder Mill Road
Adelphi, MD 20783-1197

10. SPONSORING/MONITORING AGENCY REPORT NUMBER

11. SUPPLEMENTARY NOTES
ARL PR: 9NV4VV
AMS code: 622120.H16

12a. DISTRIBUTION/AVAILABILITY STATEMENT Approved for public release; distribution unlimited.

12b. DISTRIBUTION CODE

13. ABSTRACT *(Maximum 200 words)*

Under a joint technology planning annex (TPA) agreement, fuel cell groups at the U.S. Army Research Laboratory (ARL) and the U.S. Army Communications-Electronics Command (CECOM) worked together to develop Army power sources for soldier applications. Two 50-W bipolar fuel cell stacks designed by CECOM were extensively evaluated. The performance of the stacks depended significantly on the environmental temperature. Decreasing environmental temperature granted better heat dissipation in the stacks, resulting in improved stack performance. Long-term performance of 62 W was obtained at low temperature (–5 °C). Higher environmental temperatures caused an increase in stack surface temperature. When the stack surface temperature reached 43 °C, the stack voltage dropped to zero within a short time. The maximum power density for long-term operation was 97.3 W/kg, or 167 W/L. The average hydrogen utilization efficiency was 95 percent. The water production efficiency was dependent on the discharge currents, varying from 40 percent (at 1.0 A) to 90 percent (at 2.5 A).

14. SUBJECT TERMS
Fuel cell, bipolar

15. NUMBER OF PAGES
25

16. PRICE CODE

17. SECURITY CLASSIFICATION OF REPORT	18. SECURITY CLASSIFICATION OF THIS PAGE	19. SECURITY CLASSIFICATION OF ABSTRACT	20. LIMITATION OF ABSTRACT
Unclassified	Unclassified	Unclassified	UL

NSN 7540-01-280-5500

Standard Form 298 (Rev. 2-89)
Prescribed by ANSI Std. Z39-18
298-102